

Accepted Manuscript

Title: The design of naproxen solid lipid nanoparticles to target skin layers

Author: Jafar Akbari Majid Saeedi Katayoun
Morteza-Semnani Seyyed Sohrab Rostamkalaei Masoumeh
Asadi Kofi Asare-Addo Ali Nokhodchi



PII: S0927-7765(16)30400-3
DOI: <http://dx.doi.org/doi:10.1016/j.colsurfb.2016.05.064>
Reference: COLSUB 7913

To appear in: *Colloids and Surfaces B: Biointerfaces*

Received date: 22-2-2016
Revised date: 20-5-2016
Accepted date: 24-5-2016

Please cite this article as: Jafar Akbari, Majid Saeedi, Katayoun Morteza-Semnani, Seyyed Sohrab Rostamkalaei, Masoumeh Asadi, Kofi Asare-Addo, Ali Nokhodchi, The design of naproxen solid lipid nanoparticles to target skin layers, *Colloids and Surfaces B: Biointerfaces* <http://dx.doi.org/10.1016/j.colsurfb.2016.05.064>

This is a PDF file of an unedited manuscript that has been accepted for publication. As a service to our customers we are providing this early version of the manuscript. The manuscript will undergo copyediting, typesetting, and review of the resulting proof before it is published in its final form. Please note that during the production process errors may be discovered which could affect the content, and all legal disclaimers that apply to the journal pertain.

The design of naproxen solid lipid nanoparticles to target skin layers

Jafar Akbari¹, Majid Saeedi², Katayoun Morteza-Semnani³, Seyyed Sohrab

Rostamkalaei⁴, Masoumeh Asadi⁴, Kofi Asare-Addo⁵, Ali Nokhodchi^{6,7,*}

¹ Associate Professor, Department of Pharmaceutics, Faculty of Pharmacy, Mazandaran University of Medical Sciences, Sari, Iran; ²Professor, Department of Pharmaceutics, Faculty of Pharmacy, Mazandaran University of Medical Sciences, Sari, Iran; ³Professor, Department of Medicinal Chemistry, Faculty of Pharmacy, Mazandaran University of Medical Sciences, Sari, Iran; ⁴Pharmacy Student, Department of Medicinal Chemistry, Faculty of Pharmacy, Mazandaran University of Medical Sciences, Sari, Iran; ⁵Pharmacy Department, School of Applied Sciences, University of Huddersfield, Queensgate, Huddersfield, UK; ⁶Pharmaceutics Research Laboratory, School of Life Sciences, University of Sussex, Brighton, BN1 9QJ, UK; ⁷Drug Applied Research Center and Faculty of Pharmacy, Tabriz Medical Sciences University, Tabriz, Iran.

Total number of words: 4543 (including references)

Total number of tables: 1

Total number of figures: 6

*Corresponding authors: Ali Nokhodchi, PharmD, PhD, e-mail: a.nokhodchi@sussex.ac.uk; tel: +44 1273 872811

Highlights

- Naproxen solid lipid nanoparticles (Nap-SLN) can successfully be prepared by ultrasonication
- Properties of these nanoparticles can be optimized by lipid concentrations
- HLB of the surfactants played a crucial effect on properties of solid lipid nanoparticles
- Nap-SLN increased the drug concentration in skin layer rather than systemic absorption

Abstract

The aim of the current investigation was to produce naproxen solid lipid nanoparticles (Nap-SLNs) by the ultrasonication method to improve its skin permeation and also to investigate the influence of Hydrophilic-lipophilic balance (HLB) changes on nanoparticles properties. The properties of obtained SLNs loaded with naproxen were characterized by photon correlation spectroscopy (PCS), transmission electron microscopy (TEM) and differential scanning calorimetry (DSC). FT-IR was also used to investigate any interaction between naproxen and the excipients used at the molecular level during the preparation of the SLNs. The performance of the formulations was investigated in terms of skin permeation and also the retention of the drug by the skin. It was found that generally, with increasing the lipid concentration, the average particle size and polydispersity index (PDI) of SLNs increased from 94.257 ± 4.852 nm to 143.90 ± 2.685 nm and from 0.293 ± 0.037 to 0.525 ± 0.038 respectively. The results also showed that a reduction in the HLB resulted in an increase in the PDI, particle size, zeta potential and entrapment efficiency (EE %). DSC showed that the naproxen encapsulated in the SLNs was in its amorphous form. The peaks of prominent functional groups of naproxen were found in the FT-IR spectra of naproxen-SLN, which confirmed the entrapment of naproxen in the lipid matrix. FT-IR results also ruled out any chemical interaction between drug and the chemicals used in the preparation of SLNs. The amount of naproxen detected in the receptor chamber at all the sampling times for the reference formulation (naproxen solution containing all surfactants at pH 7.4) was higher than that of the Nap-SLN8 formulation. Nap-SLN8 showed an increase in the concentration of naproxen in the skin layer with less systemic absorption. This indicates that most of the drug in Nap-SLN8 remains in the skin which can reduce the side effect of systemic absorption of the drug and increases the concentration of the drug at the site of the action.

Keywords: Naproxen, Solid lipid nanoparticles, Ultrasonication, DSC, FT-IR, Skin permeation

1. Introduction

The development of new drugs alone **is** not sufficient to ensure progress in drug therapy [1]. To overcome problems such as poor absorption, rapid metabolism and elimination, poor water solubility and high fluctuation of plasma levels, development of suitable drug delivery systems is a good strategy [2]. Naproxen is a non-steroidal anti-inflammatory drug (NSAID) which is used with increasing frequency in the treatment of rheumatic diseases and related painful conditions [3]. Naproxen protein binding in plasma is high and also varied [4] and like other NSAIDs causes gastritis and peptic ulceration after oral administration [5]. If these drugs are administered topically they should be able to provide high concentration of the drug locally if the poor permeability of the stratum corneum is overcome [6]. In order to avoid the irritation of **the** gastrointestinal tract and minimizing the systemic toxicity, application of polymer-based nanoparticles such as PLGA and eudragit RL100 with controlled drug release pattern could be useful in the treatment of inflammatory diseases [7, 8]. One of the other promising methods to reduce the side effect of naproxen is the topical administration route. Transdermal drug delivery systems provide the most important route to achieve these goals [9]. The transdermal delivery system enable controlled or sustained release of the active ingredients and also an enhanced patient compliance [10]. Topical drug delivery however, is still a challenge in pharmaceuticals and drug delivery due to the difficulties in controlling and determining the exact amount of drug that reaches the different skin layers [11]. The Active Pharmaceutical Ingredient (API) as well as the vehicle's physicochemical behaviour remains the main factors responsible for the drug differential distribution in the skin [12-14].

The bioavailability of naproxen via the percutaneous absorption is poor [15, 16] thus different technologies such as the pro-drug approach [6, 17, 18] and use of penetration enhancers in

appropriate vehicles [19] have been adopted to overcome the penetration issue of naproxen through the skin.

Recently, Solid Lipid Nanoparticles (SLN) features have been considered advantageous for topical administration of active substances. The great potential of SLN to improve prednicarbate absorption through the skin was demonstrated [20] . Another recent study reported that triptolide topical anti-inflammatory therapy was favoured by its entrapment in SLN. This strategy guaranteed an improved availability of the drug at the site of action, reducing the contemporary needed dose and thus, dose dependent side effects like irritation and staining [21] .

SLNs introduced in 1991 [22], have emerged as an alternative colloidal carriers due to advantages such as improved physical stability, good tolerability, efficient incorporation of lipophilic drugs in the lipid core of the SLNs and ease of scale up and manufacturing [23]. These nanoparticles possess a solid lipid core matrix that is solubilized by surfactants [24].

Puglia et al., showed that SLNs containing naproxen could be used as a platform for prolonged topical delivery to the skin and thus enhancing the anti-inflammatory effect of the drug [25]. They however did not investigate how the changes in HLB of the system using different proportions of binary mixtures of two surfactants with different HLB values during the preparation of the nanoparticles can change the physicochemical properties of SLNs. The aim therefore of the current study was to produce naproxen solid lipid nanoparticles to improve its skin permeation and to fully characterize them. To the best of our knowledge there is no study that has investigated the two faces of HLB in the optimization of SLNs as such this is where the novelty of the present study lies.

2. Materials and Methods

2.1 Materials

Naproxen (Nap) was purchased from Alborz bulk Co. (Tehran, Iran). Tween 80 (Samchun Pure Chemical Co., Ltd. Korea), Span 80 (Daejung Chemicals & Metals Co., Ltd. Korea), glyceryl mono stearate (GMS, (Merck Co., Germany)) were used. Distilled water was purified using a Milli-Q system (Millipore, Direct-Q).

2.2 Preparation of NAP-SLN

Naproxen nanoparticles were prepared using the probe ultrasonication method, which has been used previously for the production of lipid nanoparticles [24]. The mixture of GMS with naproxen was melted at below 100 °C using a heater stirrer. The heated mixture of solid lipid and naproxen was then mixed with 80 mL of pre-heated surfactant solution (Tween and Span mixture in percentages as in table 1 in 80 mL water) to form a pre-emulsion. The mixture was then sonicated for 10 min at 95 °C using a probe sonicator (Bandelin, Germany). Since this step is carried out at a temperature greater than the melting point of the lipid, at this stage nanoemulsion can be present due to the liquid state of the lipid. The mixture was then immersed in an ice bath instantly after the sonication process finished. This cooling step promoted the formation of the solid lipid nanoparticles. For more details of the composition readers are directed to Table 1.

2.3 Physicochemical characterization

SLNs were characterized in terms of mean particle size, polydispersity index (PDI) and zeta potential (ZP). Briefly, Zeta potential and poly dispersity index (PDI) of the nanoparticle formulations were determined using Zetasizer (Nano ZA, Malvern Instruments, UK). In this method the sample was measured at 25 °C with an angle detection of 90°. The concentration

of the samples for analysis on the Zeta Sizer was 20-400 kilo counts per second (KCPS) and the intensity of diffraction was 100000 counts per second.

2.4 Entrapment efficiency

To determine the entrapment efficiency (EE %) of Nap in the SLNs, the Nap-SLNs were subjected to centrifugation for 90 min at 29,000 rpm (HERMLE, Z36HK, Germany), filtered (pore size: 0.22 μm) and the amount of Nap in supernatant (free drug) was determined by HPLC Agilent 1100 at 230 nm, which was equipped with the Agilent Eclipse XDB-C18 column (5 μm , 4.6 \times 250 mm). The mobile phase, composed of 40:20:40 acetonitrile, methanol and acetic acid (1% v/v) was delivered at 0.7 ml/min. The retention time of the drug was 11 min. Drug entrapment efficiency (EE %) was calculated using equation 1:

$$EE\% = \frac{W_{initial\ drug} - W_{free\ drug}}{W_{initial\ drug}} \times 100 \quad (\text{Equation 1})$$

Where $W_{initial\ drug}$ is the amount of drug added in the formulation and $W_{free\ drug}$ is the amount of drug in supernatant [26].

2.5 Transmission Electron Microscopy (TEM)

TEM (Hitachi H-7500, Japan) was used for morphological observation and operated at 120 kV. Briefly, SLN samples were first diluted two times with distilled water. One drop of the diluted sample was placed on a 200-mesh carbon-coated copper grid, stained with 2 % phosphotungstic acid solution and dried at room temperature. Representative images of each sample were reported.

2.6 Fourier Transforms Infrared (FT-IR) analysis

The optimized formulations were freeze-dried and converted into solid form. A Perkin Elmer FT-IR spectrophotometer (Perkin FTIR-One, USA) was used to identify any changes in the molecular levels of naproxen, GMS, Physical mixture and Nap-SLNs from 400 to 4000 cm^{-1} . The sample was grounded with KBr and compressed into a suitable-size disk (13 mm) for measurement [26].

2.7 Differential Scanning Calorimetry (DSC)

Thermal behaviors of samples were studied by differential scanning calorimetry (Pyris 6, PerkinElmer, USA). Prior to heating, approximately 7 mg samples were equilibrated in the DSC pan (hermetic crimped aluminum pans) at 20 °C for 30 min and then heated to 250 °C at a scanning rate of 10 °C/min under N₂ atmosphere.

2.8 Powder X-ray Diffractometer (PXRD) analysis

Bruker D8 Advance X-ray diffractometer (Germany) (40 kV, 30 mA) was used to identify any changes in the crystal lattice of the materials used in making SLN. PXRD studies were performed on the samples Nap, GMS, physical mixture of Nap: GMS and Lyophilized optimized SLN by exposing them to Cu K α radiation with a wavelength of 1.5406 Å and scanned from 4.000° to 75.000°, 2 θ at a step size of 0.040° and step time of 1 s.

2.9 *In vitro* skin permeation study

The abdominal skin of Wistar male rats, weighing 200-250 g, were shaved. The abdominal skin was surgically excised. To remove the adhering subcutaneous debris and leachable enzymes, the dermal side of the skin was put in contact with a saline solution for 24 h before starting the diffusion experiment. A system employing three improved Franz diffusion cells

was used for permeation studies. The excised rat skin was set in place with the stratum corneum facing the donor compartment and the dermis facing the receptor [27]. The receiver compartment was filled with 5.5 ml of 50:50 ethanol/water mixture. The diffusion cells were maintained at 37 ± 0.5 °C with stirring at 300 rpm throughout the experiment. 10 ml of Nap-SLNs formulation as sample and naproxen solution in phosphate buffer saline (pH= 7.4) with equal amount of components except lipid as control was selected.

Samples from the receiver medium were withdrawn at predetermined time intervals (2, 4, 6, 8 and 24 h) and an equivalent volume of the medium maintained at 37 °C was replaced. All samples were filtered through 0.22 µm filters and analyzed by the HPLC method as described before in section 2.4. At the end of the permeation study, to calculate the amount of Nap deposited within the skin, the skins were removed and washed three times with phosphate buffer solution (PBS, pH 7.4) and the residual washing solvent was carefully wiped off from the skin. The skins were minced, transferred to a test tube and digested for 24 h in a 50:50 ethanol/water mixture and then sonicated for 1 h with a bath sonicator. The supernatant was then filtered through a 0.22 µm membrane and quantified by HPLC at 230 nm for Nap content.

2.10 Statistical analysis

All the results are expressed as the mean \pm standard deviation of at least three determinations (n=3). The treated groups were compared to the control by analysis of variance (ANOVA), following Tukey test. In the case of comparison of only two means, t-test was performed. The statistical analysis was carried out using the SPSS software. A P-value < 0.05 was considered as significant.

3. Results and discussion

3.1 Effect of drug/lipid ratio on nanoparticle characterization

The composition of the SLN formulations and their properties are listed in Table 1. It was found that, generally, an increase in the lipid concentration, brought about an increase in the particle size and PDI of SLNs ($P < 0.001$) (compare Nap-SLN1 with Nap-SLN3 in Table 1). Jameel *et al.* also indicated that an increase in lipid level showed a significant influence upon particle size [28]. The results are as such in agreement with previous research studies [28, 29]. However, in another study on SLN loaded with meloxicam, an increase in lipid concentration was associated with an increase in particle size, but only when the lipid concentration exceeded a critical value [30]. Vitorino *et al.* showed that, higher lipid content in each initial dichloromethane (DCM) droplet also promotes larger particles after solvent evaporation [31]. The drug entrapment efficiency of Nap-SLNs (Nap-SLN1 to Nap-SLN3) varied from 59.46 to 66.34 % (Table 1). The lowest EE % belonged to the formulations containing high concentration of lipid. This could be due to the partial expulsion of the drug at the particle surfaces during the crystallization of the lipid phase leading to lower EE %. Furthermore, when the concentration of lipid in the formulation is high, this increases the viscosity at the interface (between lipid phase and aqueous phase). The increase in the viscosity can slow down the diffusion of lipid particles into the aqueous phase [32] leading to low EE %.

3.2 Effect of HLB on nanoparticles characterization

The results of the effect of HLB showed that a reduction in the HLB of the surfactants causes an increase in the PDI (wider size distribution), particle size, zeta potential (a better stability) and EE % (Table 1). As the main goal of the present study was to manufacture SLNs with a better stability, high entrapment efficiency, smaller particles and a narrow sized distribution,

different HLB values (between 8 and 16) in the system were produced by using different proportion of binary mixtures of two surfactants with two different HLBs, in order to find the optimum values of HLB that can fulfill the above mentioned requirements such as size, PDI, EE % and zeta potential. Higher EE % may be as a result of the high solubility of naproxen in span 80 [33]. In order to decrease the HLB value of the system, the amount of Span 80 (the surfactant with low HLB) should increase, therefore span 80 helps to load naproxen into the solid lipid. It is generally expected that the smallest emulsion droplets can be obtained when the optimum HLB level is attained during the manufacturing process. This could explain why the smallest particles with the narrower distribution were obtained for Nap-SLN4. This in turn can increase the stability of the formulations when binary mixtures of surfactants are used. The use of binary mixtures of surfactants with low and high HLB ensure a better stability of emulsion droplets as the surfactant with high HLB can be dispersed in aqueous phase and the one with low HLB can be dispersed in oily phase leading to the stability of the surfactant film at the interface from the reservoir created in each phase [9]. The values of zeta potential reduced as the HLB value of the system reduced. Beyond the optimum HLB value the zeta potential of the particles increased significantly. Although Tween 80 and Span 80 are non-ionic surfactants, the zeta potential of the droplets has gone up to -10.5 mV which could be due to residual electrolyte coming from the ethoxylation catalyst described by Abismail, et al., [34] and this effect increases with an increase in the span 80 concentration.

3.3 TEM analysis

In order to show microscopy images of nanoparticles, Nap-SLN6 was selected as one of the formulations with narrower distribution and its microscope image is presented in Figure 1. This image reveals that the particles were segregated, uniform in size and spherical in shape. The particle size observed by TEM imaging technique was less than dynamic light scattering

technique using zeta-sizer probably because the nanoparticles get dehydrated while preparing for TEM analysis. Zetasizer tends to measure the apparent diameter of the particles, including the hydrodynamic layers surrounding the particles, resulting in an overestimated particle size [35].

3.4 FT-IR

Figure 2 illustrates the infrared spectra of naproxen, GMS, Nap-SLN6 and physical mixture (with the same composition). Nap shows diagnostic bands at 3193 cm^{-1} (OH, stretching), 2939 cm^{-1} (C-H, stretching), 1728 cm^{-1} (non-hydrogen-bonded C=O , stretching), 1684 cm^{-1} (hydrogen-bonded C=O , stretching), 1604 cm^{-1} and $1504\text{--}1453\text{ cm}^{-1}$ (aromatic C=C , stretching), 1264 cm^{-1} (Aryl-O, asymmetric stretching), 1091 cm^{-1} (C-O, stretching) and 1029 cm^{-1} (Aryl-O, symmetric stretching). Some of these diagnostic bands (e.g., 1605 cm^{-1} and 1028 cm^{-1}) were found in Nap-SLN6 or in the physical mixture formulation but with smaller intensity due to less concentration of naproxen in the formulation compared to pure naproxen. GMS shows bands at $3400\text{--}3200\text{ cm}^{-1}$ (OH, stretching), $3000\text{--}2850\text{ cm}^{-1}$ (C-H, stretching), 1731 cm^{-1} (C=O , stretching) and $1300\text{--}1000\text{ cm}^{-1}$ (C-O, stretching). Both naproxen and GMS have carbonyl groups peaks which shifted and were almost overlapped. The peak shifts were small, two peaks were near to each other but still recognizable, which revealed entrapment of naproxen in lipid matrix. FT-IR results also proved no chemical interaction between drug and its carriers. Similar conclusion was drawn for other formulations.

3.5 Differential scanning calorimetry (DSC)

The pure naproxen, bulk GMS, the physical mixture and Nap-SLNs powder were examined by DSC and their DSC traces are shown in Figure 3. Naproxen showed a single sharp endothermic melting peak at about $154\text{ }^{\circ}\text{C}$ corresponding to its melting point, indicating its

characteristic crystalline nature. Bulk GMS showed a single endothermic melting peak around 56-67 °C. As observed in Figure 3, the DSC trace of Nap-SLN6 and its physical mixture contained the endothermic peak around the GMS melting point. The endothermic peak of crystalline form of drug disappeared. This suggests conversion of crystalline naproxen to the amorphous form which could be attributed to complete dissolution of the drug in the molten lipid matrix. This phenomenon was also true for all the Nap-SLN formulations investigated.

3.6 Powder X-ray Diffractometer (PXRD) analysis

Figure 4 shows the X-ray diffraction (PXRD) pattern of Nap. Nap manifested the distinct peaks at 2θ : 6.5°, 12.4°, 16.6°, 19°, 20°, 22.5°, 24° and 28.5° indicating the highly crystalline nature of the drug. The PXRD pattern of GMS showed a peak at about 20°, indicating the crystalline nature of the lipid. In case of Nap-SLN the principal peak of naproxen is absent in PXRD spectra (Figure 4). Furthermore, the principal peak of lipid did not shift but had a reduced intensity as compared to the free lipid. This may be attributed to the incorporation of naproxen between the parts of the lipid, leading to a change in the crystallinity of the Nap-SLNs.

3.8 *In vitro* percutaneous absorption study

Rat skin was used in the percutaneous absorption study. Although it has been widely reported that the human skin can provide more reliable skin absorption data compared to rat skin [36-37], such studies most of the time is not feasible particularly during the initial development of a novel pharmaceutical formulation. In addition, it is generally accepted that the human skin is less permeable than rat skin [38], however, as this study aimed to determine the performance of the formulation made with that of previous

studies where the rat skin model was used, the authors therefore opted to use the rat skin model also to allow for such a comparison to be made. Figures 5 and 6 shows the cumulative plots of the amount of naproxen that penetrated through rat skin (transdermal delivery) as a function of time and the amount of naproxen that penetrated to the skin layers (dermal delivery) respectively. In order to evaluate the skin targeting potential of SLN, the permeation ability of Nap into and through the skin was evaluated using Franz diffusion cells. The solution containing 0.0625 % naproxen, 0.851 % Tween 80 and 1.149 % Span 80 (similar to SLN8 formulation) in phosphate buffer (pH=7.4) was used as the standard to evaluate the skin permeation and skin absorption versus the Nap-SLN8 formulation. The amount of Nap measured in the receptor chamber for the reference formulation was higher than when nanoparticle formulation (Nap-SLN8) was used ($p<0.05$) (Figure 5), whereas the amount of Nap remaining in the skin layers for nanoparticle formulation (Nap-SLN8) was much higher than the reference formulation ($p<0.05$)(Figure 6). This highlights the property of the Nap-SLN8 formulation to decrease systemic uptake and systemic adverse effects and thus improving the drug levels achieved at the site of disease. Furthermore, a prolonged anti-inflammatory effect could be shown for drug loaded SLNs compared to drug solution [25, 39]. Francesco *et al* also showed that the use of SLN can improve the oil accumulation of the formulation into the skin, while in case of the control solution (conventional formulation) the oil permeation occurred through the skin (less oil in the skin layers) [40]. Puglia *et al* also demonstrated that the particles were able to reduce the drug penetration, but increasing, simultaneously, the permeation and the accumulation in the horny layer [25]. These researchers showed that the anti-inflammatory effect drugs can be prolonged in the case of drug loaded nanoparticles compared to the drug solution [25]. The results obtained in the present study and the *in vivo* data published previously demonstrated that lipid nanoparticles are promising in drug delivery and stimulating new and deeper investigations in the field.

4. Conclusion

The present study showed that solid lipid nanoparticles loaded with naproxen can be successfully manufactured using the probe ultrasonication technique and could be suitable carriers for the skin and for the local delivery of naproxen. It has been shown previously that SLNs increase the dermal delivery of the drug with a less delivery of the drug into deeper layers of the skin for systemic absorption. **The results showed that SLN formulation can increase the concentration of the drug at the top layers of the skin compared to the drug solution formulation containing the same components as the SLN.** The results showed that a reduction in HLB increased PDI, particle size, zeta potential and the entrapment encapsulation. This indicates that the HLB value of the surfactants used in the manufacture of SLNs can thus control the physiochemical properties of SLNs to achieve the desired properties. The present study emphasizes that the concentration of naproxen in the skin layers is higher when SLNs were used compared to the reference formulation (naproxen solution containing all surfactants). Solid state analysis also showed that naproxen was in its amorphous state in the nanoparticle formulations.

Acknowledgments

This work was supported by a grant from the research council of Mazandaran University of Medical Sciences.

References

- [1] J. You, F. Wan, F. de Cui, Y. Sun, Y.Z. Du, F.Q. Hu, *Int.J. Pharm.*, 343 (2007) 270-276.
- [2] K.A. Shah, A.A. Date, M.D. Joshi, V.B. Patravale, *Int. J. Pharm.*, 345 (2007) 163-171.
- [3] P.A. Todd, S.P. Clissold, *Drugs*, 40 (1990) 91-137.
- [4] H. Held, *Arzneimittel-Forschung*, 30 (1980) 843-846.
- [5] R.N. Brogden, R.C. Heel, T.M. Speight, G.S. Avery, *Drugs*, 18 (1979) 241-277.
- [6] H. Weber, U. Steimer, R. Mannhold, G. Cruciani, *Pharm. Res.*, 18 (2001) 600-607.
- [7] K. Adibkia, Y. Javadzadeh, S. Dastmalchi, G. Mohammadi, F.K. Niri, M. Alaei-Beirami, *Colloids and Surfaces B: Biointerfaces*, 83 (2011) 155-159.

- [8] Y. Javadzadeh, F. Ahadi, S. Davaran, G. Mohammadi, A. Sabzevari, K. Adibkia, *Colloids Surf. B: Biointerfaces*, 81 (2010) 498-502.
- [9] D. Attwood, A.T. Florence, *Fast Track: Physical Pharmacy*, Pharmaceutical Press 2008.
- [10] D.B. Troy, J.P. Remington, P. Beringer, *Remington: The Science and Practice of Pharmacy*, Lippincott Williams & Wilkins 2006.
- [11] M. Schäfer-Korting, W. Mehnert, H.-C. Korting, *Adv. Drug Del. Rev.*, 59 (2007) 427-443.
- [12] E. Beetge, J. du Plessis, D.G. Müller, C. Goosen, F.J. van Rensburg, *Int. J. Pharm.*, 193 (2000) 261-264.
- [13] U. Jacobi, T. Tassopoulos, C. Surber, J. Lademann, *Archives Dermatol. Res.*, 297 (2006) 303-310.
- [14] A. Teichmann, S. Heuschkel, U. Jacobi, G. Presse, R.H. Neubert, W. Sterry, J. Lademann, *Eur. J. Pharm. Biopharm.*, 67 (2007) 699-706.
- [15] P. Singh, M. Roberts, *J. Pharmacol. Exp. Therapeutics*, 268 (1994) 144-151.
- [16] H. Suh, H.W. Jun, M. Dzimianski, G. Lu, *Biopharm. Drug Dispos.*, 18 (1997) 623-633.
- [17] F. Bonina, L. Montenegro, F. Guerrera, *Int. J. Pharm.*, 100 (1993) 99-105.
- [18] J. Rautio, T. Nevalainen, H. Taipale, J. Vepsäläinen, J. Gynther, K. Laine, T. Järvinen, *Eur. J. Pharm. Sci.*, 11 (2000) 157-163.
- [19] I. Degim, A. Uslu, J. Hadgraft, T. Atay, C. Akay, S. Cevheroglu, *Int. J. Pharm.*, 179 (1999) 21-25.
- [20] C.S. Maia, W. Mehnert, M. Schäfer-Korting, *Int. J. Pharm.*, 196 (2000) 165-167.
- [21] Z. Mei, H. Chen, T. Weng, Y. Yang, X. Yang, *Eur. J. Pharm. Biopharm.*, 56 (2003) 189-196.
- [22] D. Hou, C. Xie, K. Huang, C. Zhu, *Biomaterials*, 24 (2003) 1781-1785.
- [23] W. Mehnert, K. Mäder, *Adv. Drug Del. Rev.*, 47 (2001) 165-196.
- [24] B.-D. Kim, K. Na, H.-K. Choi, *Eur. J. Pharm. Biopharm.*, 24 (2005) 199-205.
- [25] C. Puglia, P. Blasi, L. Rizza, A. Schoubben, F. Bonina, C. Rossi, M. Ricci, *Int. J. Pharm.*, 357 (2008) 295-304.
- [26] T. Delmas, A.-C. Couffin, P.A. Bayle, F. De Crecy, E. Neumann, F. Vinet, M. Bardet, J. Bibette, I. Texier, *J. Colloid Interface Sci.*, 360 (2011) 471-481.
- [27] H. Kelidari, M. Saeedi, J. Akbari, K. Morteza-Semnani, P. Gill, H. Valizadeh, A. Nokhodchi, *Colloids Surf. B: Biointerfaces*, 128 (2015) 473-479.
- [28] J.A.S. Mulla, S.P. Hiremath, N.K. Sharma, *J. Pharm. Sci.*, 2 (2012) 41-49.
- [29] B. Siekmann, K. Westesen, *Pharm. Pharmacol. Lett.*, 3 (1994) 194-197.
- [30] R.M. Khalil, A.A. El-Bary, M.A. Kassem, M.M. Ghorab, M.B. Ahmed, *Eur. Sci. J.*, (2013).
- [31] C. Vitorino, F.A. Carvalho, A.J. Almeida, J.J. Sousa, A.A. Pais, *Colloids Surf. B: Biointerfaces*, 84 (2011) 117-130.
- [32] C. Freitas, R.H. Müller, *Int. Pharm.*, 168 (1998) 221-229.
- [33] E. Moghimipour, A. Salimi, S. Eftekhari, *Adv. Pharm. Bulletin*, 3 (2013) 63-71.
- [34] B. Abismail, J.P. Canselier, A.M. Wilhelm, H. Delmas, C. Gourdon, *Ultrasonics Sonochemistry*, 6 (1999) 75-83.
- [35] M. Fazil, S. Md, S. Haque, M. Kumar, S. Baboota, J. Kaur Sahni, J. Ali, *Eur. J. Pharm. Sciences*, 47 (2012) 6-15.
- [36] E.C. Jung, H.I. Maibach. *J. Appl. Toxicol.*, 35 (2015) 1–10.
- [37] B. Godin, E. Touitou. *Adv. Drug Del. Rev.*, 59 (2007) 1152–1161
- [38] J. Príborský, E. Mühlbachová. *J. Pharm Pharmacol.* 42 (1990) 468-72.
- [36] Z. Mei, H. Chen, T. Weng, Y. Yang, X. Yang, *Eur. J. Pharm. Biopharm.* 56 (2003) 189–196.

[37] F. Lai, C. Sinico, A. De Logu, M. Zaru, R. Muller, A.M. Fadda, *Int. J. Nanomedicine*, 2 (2007) 419.

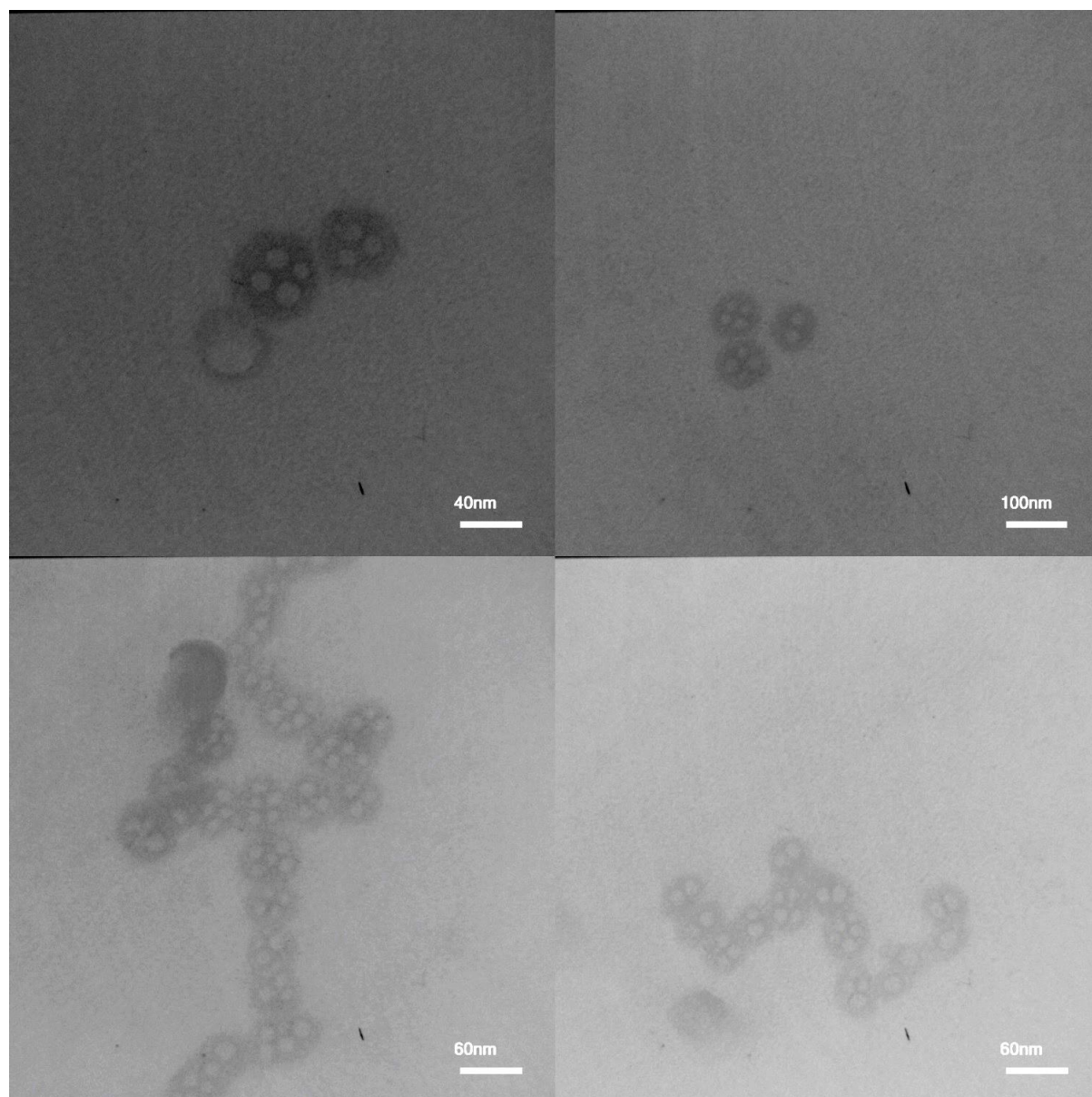


Figure 1. Various TEM micrographs of Nap-solid lipid nanoparticles (Nap-SLN6) with different magnifications.

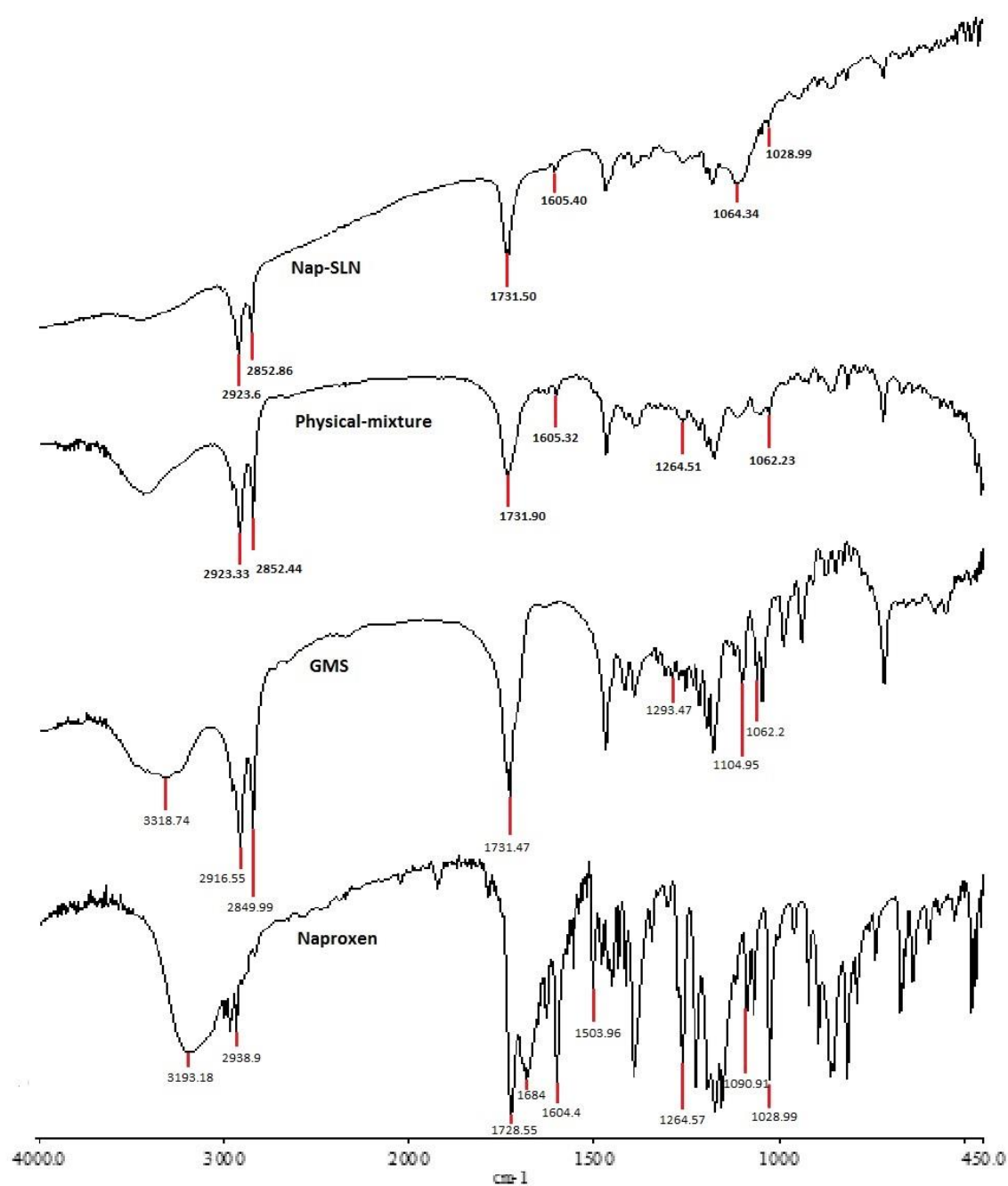


Figure 2. FT-IR spectra of naproxen, GMS, Nap-GMS physical mixture and Nap-SLN6.

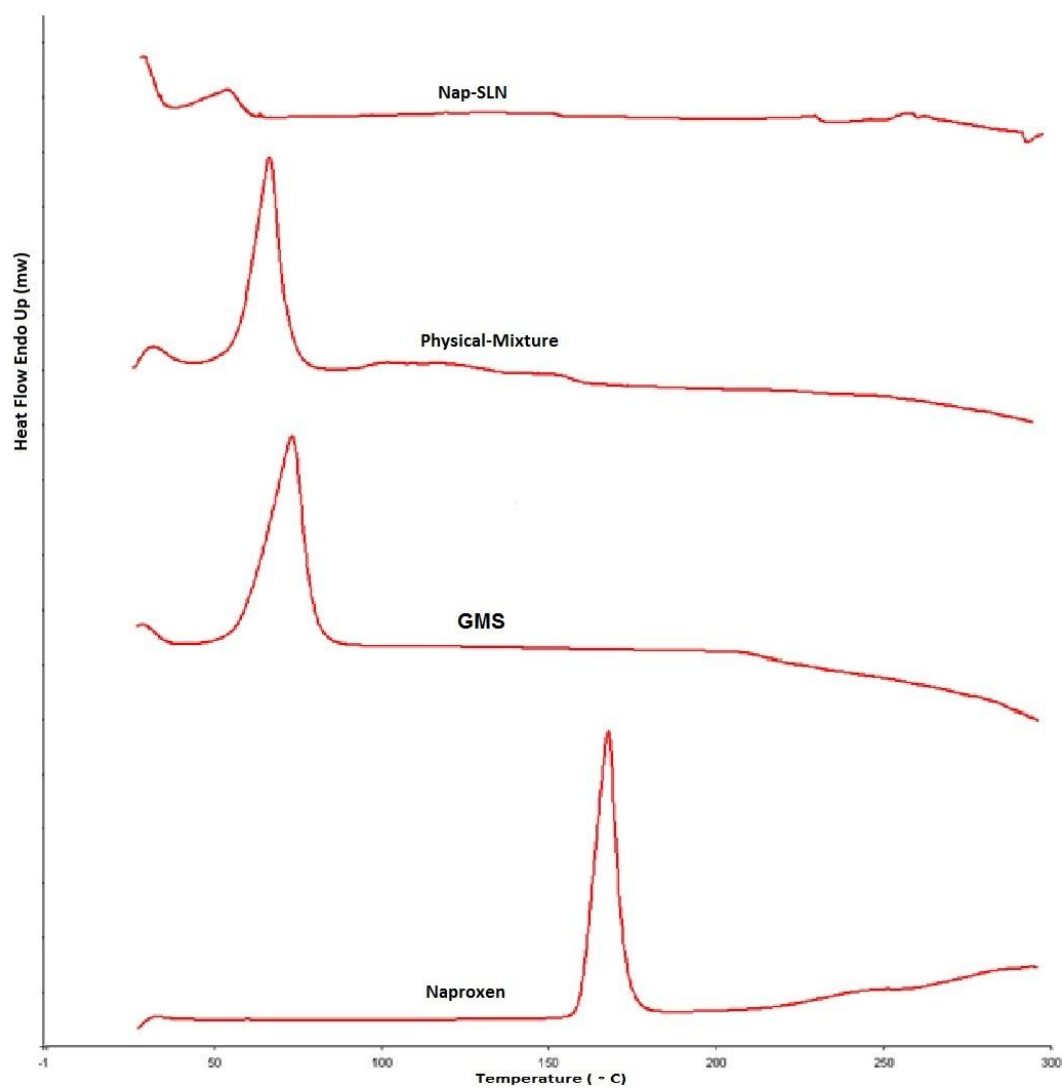


Figure 3. DSC traces of Naproxen, GMS, Nap-GMS physical mixture and Nap- SLN6.

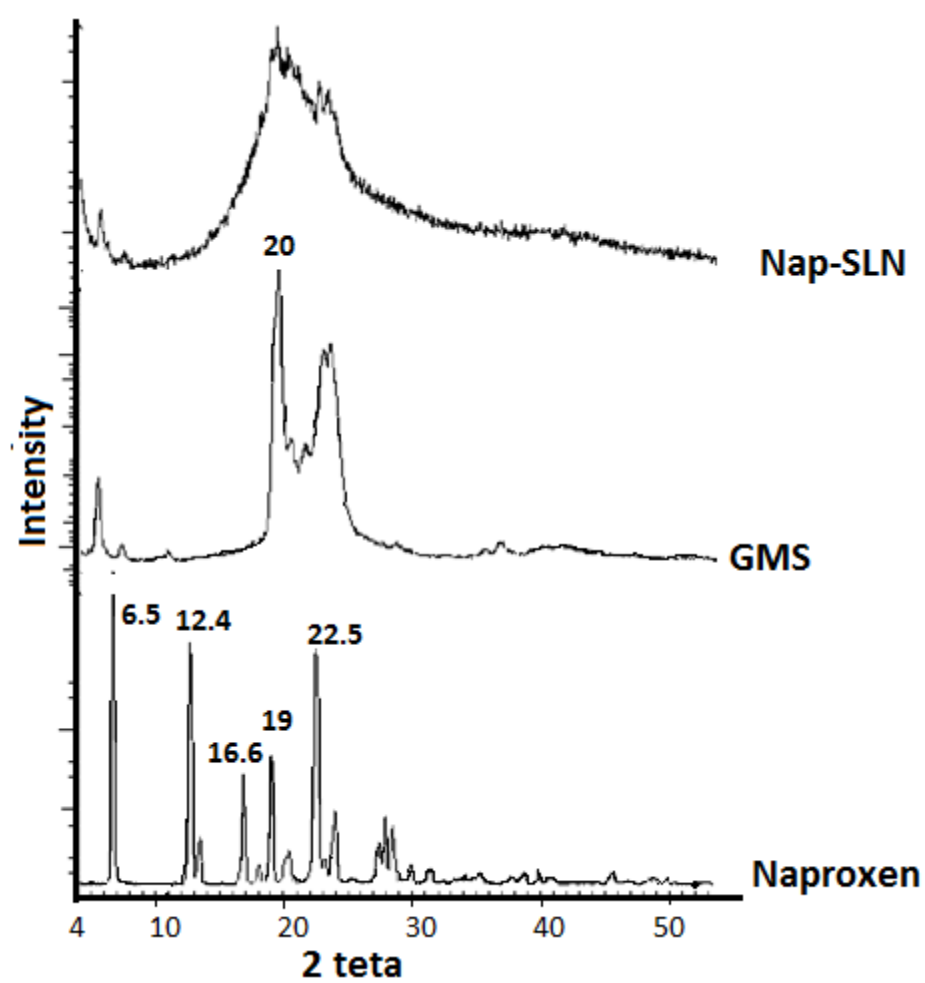


Figure 4. XRD of Naproxen, GMS and Nap-SLN6.

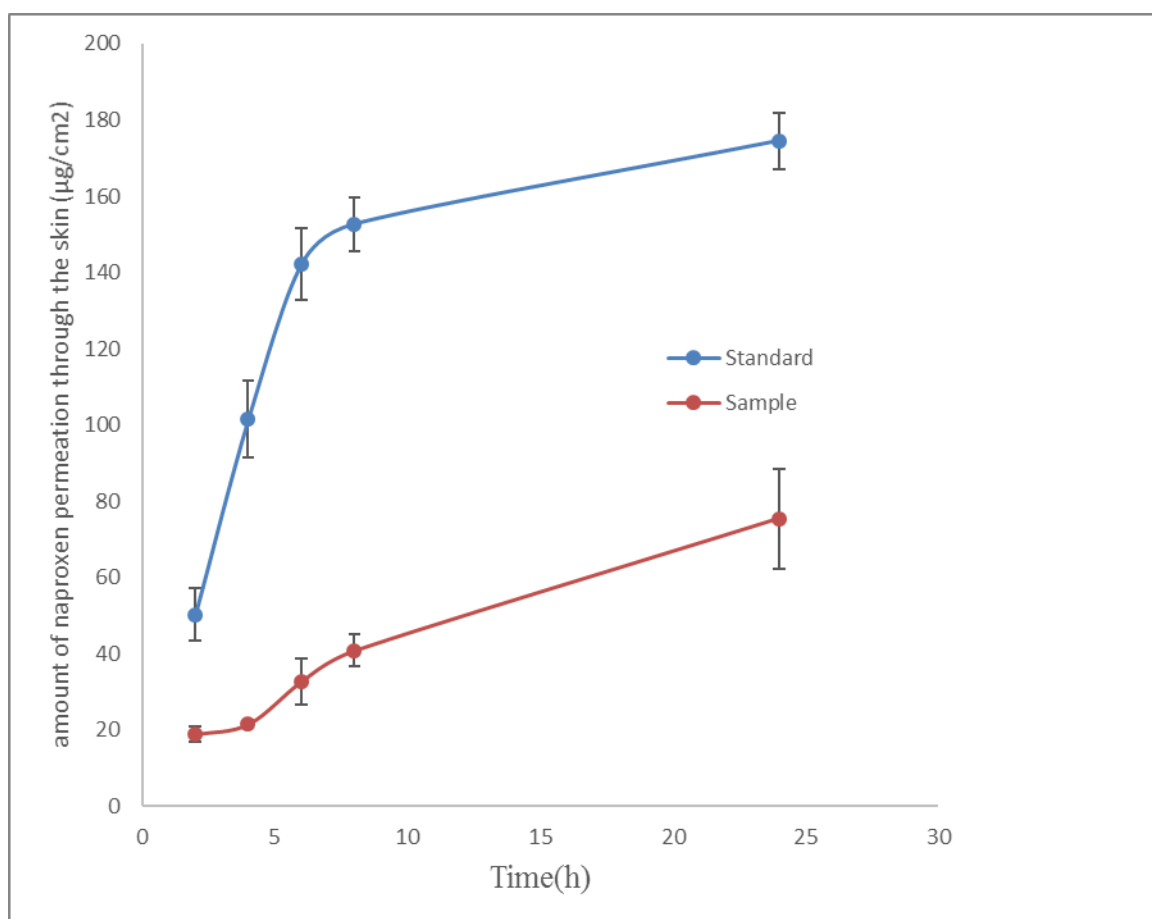


Figure 5. Cumulative amount of naproxen permeated across rat skin (data is mean and standard deviation of three determinations, $n=3$; ANOVA test followed by Tukey's test showed that the effect of time and formulation on naproxen permeation was significant $p<0.05$). Sample represents Nap-SLN8 and standard is naproxen solution containing the same concentration of surfactants used in SLN8 at pH 7.4.

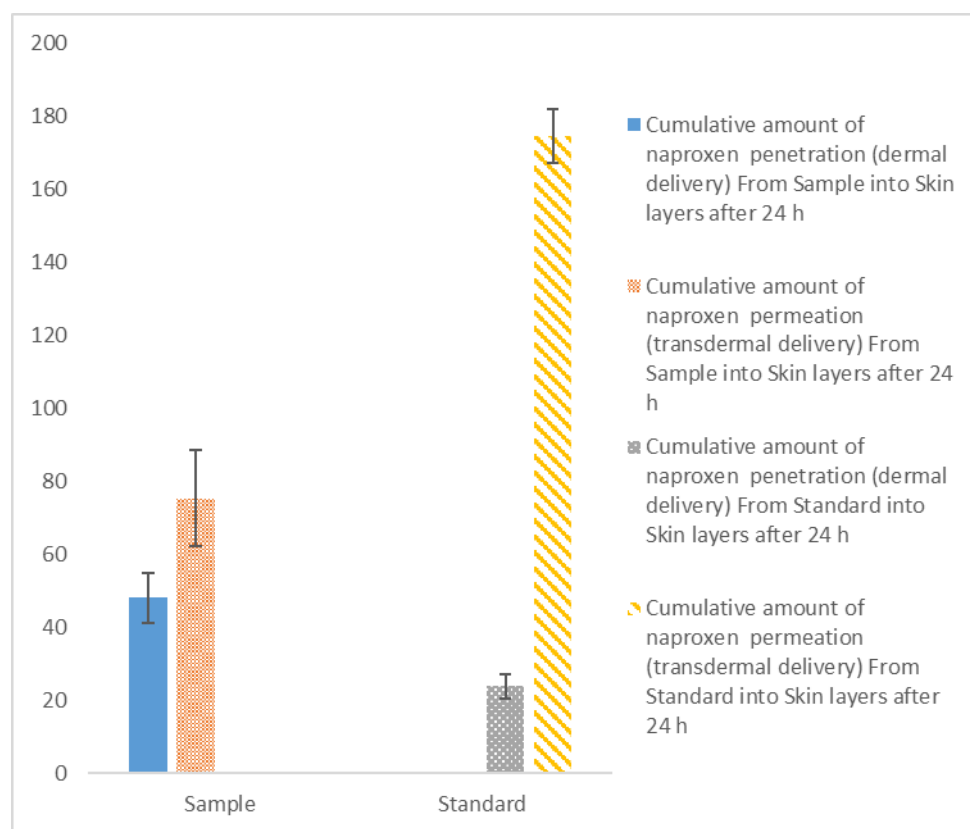


Figure 6. Amount of naproxen penetrating to the skin layers (Dermal delivery) (error bars are standard deviation, sample represents Nap-SLN8 and standard formulation is the naproxen solution at pH 7.4; t-test was carried out between the sample and standard. The difference was significant $p < 0.05$; $n = 3$).

Table 1: Component and physicochemical properties of investigated NAP-loaded SLN (% w/w). The data are the mean and standard deviation of three determinations (n=3). NAP: naproxen; GMS: glyceryl monostearate; PDI: polydispersity index; zeta potential; EE: entrapment efficiency

Formulation	Naproxen (%)	GMS (%)	Span 80 (%)	Tween 80 (%)	Water (%)	HLB	Particle Size* (nm)	PDI**	Zeta Potential** (mv)	EE%***
Nap-SLN1	0.061	0.305	0.651	1.302	Qs 100	11.4	94.3±4.9	0.293±0.037	-7.55±0.23	66.35±1.10
Nap-SLN2	0.061	0.609	0.649	1.298	Qs 100	11.4	105.5±5.2	0.404±0.012	-7.15±1.09	59.46±0.50
Nap-SLN3	0.060	1.210	0.645	1.290	Qs 100	11.4	143.9±2.7	0.525±0.038	-7.10±0.46	59.83±1.15
Nap-SLN4	0.061	0.305	-	1.954	Qs 100	14.9	84.5±2.0	0.273±0.044	-4.96±0.16	59.95±0.74
Nap-SLN5	0.061	0.305	0.210	1.744	Qs 100	13.8	100.0±9.7	0.270±0.107	-3.92±0.71	60.24±0.32
Nap-SLN6	0.061	0.305	0.488	1.465	Qs 100	12.3	140.7±18.3	0.241±0.020	-5.06±0.78	61.64±0.37
Nap-SLN7	0.061	0.305	0.814	1.115	Qs 100	10.5	162.2±24.2	0.351±0.046	-7.05±2.21	62.45±0.13
Nap-SLN8	0.061	0.305	1.122	0.831	Qs 100	8.7	252.6±43.1	0.394±0.081	-10.57±0.57	62.91±1.79

ANOVA test followed by Tukey's test showed that the effect of HLB on particle size, PDI, zeta potential and EE% was significant ($p < 0.05$). *In the particle size column all the particle sizes are significantly different from each other (Tukey's test); **The effect of HLB on PDI and zeta potential is more dominant when the difference in the HLB value is more than 1.8 (for example there is no significant difference between Nap-SLN8 and Nap-SLN7, but this difference was significant when Nap-SLN8 was compared to Nap-SLN6). ***Nap-SLN1 is significantly different from the other formulations. The difference between SLN3, SLN4, SLN5, SLN6 and SLN7 is not significant ($p > 0.05$). The difference between SLN4 with SLN8 and SLN5 and SLN8 is significant ($p < 0.05$).